



## Radiosynthesis of a $^{18}\text{F}$ -labeled 2,3-diarylsubstituted indole via McMurry coupling for functional characterization of cyclooxygenase-2 (COX-2) in vitro and in vivo

Torsten Knies <sup>a,\*</sup>, Markus Laube <sup>a</sup>, Ralf Bergmann <sup>a</sup>, Fabian Sehn <sup>a</sup>, Franziska Graf <sup>a</sup>, Joerg Steinbach <sup>a</sup>, Frank Wuest <sup>b</sup>, Jens Pietzsch <sup>a</sup>

<sup>a</sup> Institute of Radiopharmacy, Helmholtz-Zentrum Dresden-Rossendorf, Dresden, Germany

<sup>b</sup> Department of Oncology, University of Alberta, Edmonton, Canada

### ARTICLE INFO

#### Article history:

Received 8 February 2012

Revised 4 April 2012

Accepted 10 April 2012

Available online 17 April 2012

#### Keywords:

Cyclooxygenase-2

COX-2 inhibitor

$^{18}\text{F}$ -radiolabeling

McMurry cyclization

Positron emission tomography

### ABSTRACT

The radiosynthesis of 3-(4-[ $^{18}\text{F}$ ]fluorophenyl)-2-(4-methylsulfonylphenyl)-1*H*-indole [ $^{18}\text{F}$ ]-**3** as potential PET radiotracer for functional characterization of cyclooxygenase-2 (COX-2) in vitro and in vivo is described. [ $^{18}\text{F}$ ]-**3** was prepared by McMurry cyclization of a  $^{18}\text{F}$ -labeled intermediate with low valent titanium and zinc via a two-step procedure in a remote controlled synthesizer unit including HPLC purification and solid phase extraction. In this way [ $^{18}\text{F}$ ]-**3** was synthesized in 80 min synthesis time in 10% total decay corrected yield from [ $^{18}\text{F}$ ]fluoride in radiochemical purity >98% and a specific activity of 74–91 GBq/ $\mu\text{mol}$  (EOS). [ $^{18}\text{F}$ ]-**3** was evaluated in vitro using pro-inflammatory stimulated THP-1 and COX-2 expressing tumor cell lines (FaDu, A2058, HT-29), where the radiotracer uptake was shown to be consistent with up regulated COX-2 expression. The stability of [ $^{18}\text{F}$ ]-**3** was determined by incubation in rat whole blood and plasma in vitro and by metabolite analysis of arterial blood samples in vivo, showing with 75% of original compound after 60 min an acceptable high metabolic stability. However, no substantial tumor accumulation of [ $^{18}\text{F}$ ]-**3** could be observed by dynamic small animal PET studies on HT-29 tumor-bearing mice in vivo. This may be due to the only moderate COX-1/COX-2 selectivity of **3** as demonstrated by both cellular and enzymatic cyclooxygenase inhibition assay in vitro. Nevertheless, the new approach first using McMurry cyclization in  $^{18}\text{F}$ -chemistry gives access to  $^{18}\text{F}$ -labeled diarylsubstituted heterocycles that hold promise as radiolabeled COX-2 inhibitors.

© 2012 Elsevier Ltd. All rights reserved.

### 1. Introduction

Cyclooxygenase isoforms COX-1 and COX-2, also known as prostaglandin H synthases or prostaglandin endoperoxide synthases, are the key rate-limiting enzymes converting arachidonic acid into prostaglandins, prostacyclin, and thromboxanes. These bioactive lipids are involved in maintaining of physiological conditions but also in certain pathophysiological processes. COX-1 is constitutively expressed in most mammalian tissues and is responsible for thrombogenesis and homeostasis as well. COX-2 is an inducible enzyme, whose expression is stimulated by a host of inflammatory cytokines, mitogens, hormones and growth factors; consistently, COX-2 overexpression is implicated in a number of disease processes including pain, inflammation, and atherogenesis.<sup>1</sup> Furthermore, elevated COX-2 level has been reported in a wide variety of cancers, including colorectal adenocarcinoma, breast, and lung cancer.<sup>2–4</sup> COX-2 may play a key role in both

inflammogenesis and radioresistance of tumors, and consequently blocking the COX-2-mediated synthesis of eicosanoids may provide effective chemoprevention or adjuvant radiosensitizing therapy.<sup>5,6</sup> In this regard, COXs are the target of aspirin-like and other non-steroidal anti-inflammatory drugs (NSAIDs). Recently, therapeutic approaches targeting COX-related processes forward the use of selective COX-2 inhibitors (coxibs) such as celecoxib, etoricoxib, and lumiracoxib. Determination of COX-2 expression levels and/or activity in patients can currently only be achieved by invasive and laborious ex vivo analyses. Characterization of functional COX-2 expression by means of positron emission tomography (PET) would non-invasively provide information for optimization of coxibe therapy and therapy control in vivo. Furthermore, this would allow a deeper understanding of the role of COX-2 in various disorders and pathophysiological situations. Several attempts have been made to develop COX-2 inhibitors radiolabeled with positron emitters over the last decade. A number of  $^{18}\text{F}$ - and  $^{11}\text{C}$ -labeled analogs of celecoxib and related compounds with heterocyclic core have been described<sup>7–9</sup> and recently an  $^{18}\text{F}$ -labeled COX-2 inhibitor basing on a celecoxib derivative for

\* Corresponding author. Tel./fax: +49 351 2602760.

E-mail address: [t.knies@hzdr.de](mailto:t.knies@hzdr.de) (T. Knies).

imaging of inflammation and COX-2 expressing human tumor xenografts was published.<sup>10</sup> We have contributed to this field with the radiosynthesis and preliminary evaluation of derivatives of <sup>18</sup>F- and <sup>11</sup>C-labeled 1,2-diarylcyclopentenes as highly affine and selective COX-2 inhibitors.<sup>11,12</sup> Unfortunately, the results are inconsistent due to the relatively high lipophilicity of the tracers causing some kind of so-called unspecific binding and the narrow time slot for pharmacologic investigations originating from the short half-life of the <sup>11</sup>C-label.

Recently, a new series of 2,3-diarylsubstituted indoles with high affinity and selectivity has been published as supposable COX-2 inhibitors.<sup>13</sup> The heterocyclic ring system bearing the two vicinal aryl moieties substituted with a methylsulfonyl group shows the classical 'coxibe-structure', whereas the indole ring constitutes an important template for drug design.

The published IC<sub>50</sub> values of the 2,3-diarylsubstituted indoles 2-(4-aminosulfonylphenyl)-3-(4-methoxyphenyl)-1*H*-indole **1**, 3-(4-methoxyphenyl)-2-(4-methylsulfonylphenyl)-1*H*-indole **2** and 3-(4-fluorophenyl)-2-(4-methylsulfonylphenyl)-1*H*-indole **3** obtained in COX-2 enzyme-binding assays were in the low nanomolar level in addition with high COX-1/COX-2 selectivity ratios (Fig. 1). The lipophilicity is in acceptable range on account of the heterocyclic moiety; so for compound **3** a log*P* was calculated to be about 2.3 ± 0.7 (ACDLab<sup>®</sup>) a value that is expected to diminish the unspecific binding of the corresponding radiotracer.

Lately compound **1** has been successfully radiolabeled with carbon-11 by reaction of the hydroxyl-precursor with <sup>11</sup>C-methyltriflate and the radiopharmaceutical behavior has been explicitly studied.<sup>14</sup> The authors found [<sup>11</sup>C]-**1** to be relatively unstable with 54% of intact compound in plasma 30 min post injection, furthermore [<sup>11</sup>C]-**1** was suspected to be a substrate for the P-glycoprotein efflux pump. With respect to the limitations of <sup>11</sup>C-radiochemistry discussed above, we focused on a labeling of the 2,3-diarylsubstituted indole system with [<sup>18</sup>F]fluorine. In this paper we report on the radiosynthesis of 3-(4-[<sup>18</sup>F]fluorophenyl)-2-(4-methylsulfonylphenyl)-1*H*-indole [<sup>18</sup>F]-**3**, via McMurry cyclization, a labeling approach that has not been described so far. Pharmacological characterization of [<sup>18</sup>F]-**3** was performed in human leukemic monocyte cell line (THP-1) as well as human solid tumor cell lines (FaDu, HT-29, and A2058) as models for upregulated COX-2 expression in vitro. Stability experiments were accomplished in rats and in vivo dynamic small animal PET studies in tumor-bearing mice.

## 2. Experimental

### 2.1. Materials and methods

All commercial reagents and solvents were used without further purification unless otherwise specified. Nuclear magnetic

resonance spectra were recorded on a Unity 400 MHz spectrometer (Varian). <sup>1</sup>H NMR chemical shifts were given in ppm and were referenced with the residual solvent resonances relative to tetramethylsilane (TMS). Mass spectra were obtained on a Quattro/LC mass spectrometer (Micromass) by electrospray ionization. Flash chromatography was conducted using MERCK silica gel (mesh size 230–400 ASTM). Thin-layer chromatography (TLC) was performed on Merck silica gel F-254 aluminum plates with visualization under UV (254 nm). No-carrier-added aqueous [<sup>18</sup>F]fluoride was produced in a CYCLONE 18/9 cyclotron (IBA) by irradiation of [<sup>18</sup>O]H<sub>2</sub>O via the <sup>18</sup>O(p,n)<sup>18</sup>F nuclear reaction.

Synthesis of 3-(4-[<sup>18</sup>F]fluorophenyl)-2-(4-methylsulfonylphenyl)-1*H*-indole [<sup>18</sup>F]-**3** and semi-preparative purification was performed in an automated nucleophilic synthesizer TracerLab<sup>®</sup>FXN (GE). Semi-preparative HPLC purifications were carried out with a Nucleodur-Isis C18 column (250 × 10 mm, 5 μm, Macherey-Nagel) using an isocratic eluent of acetonitrile/water = 70:30 by a S1122 HPLC-pump (Sykam) with a flow rate of 4 mL/min. The product was monitored by a K-2001 filter photometer (Knauer) at 254 nm and by a gamma-detector integrated in the synthesizer module. Analytical HPLC analysis was carried out with a C18 column (Nucleodur-Isis, 250 × 4 mm, 5 μm, MN) using an isocratic eluent of acetonitrile/water 0.1%TFA = 70:30 by a gradient pump L2500 (Merck, Hitachi) with a flow rate of 1 mL/min. The products were monitored by an UV detector L4500 (Merck, Hitachi) at 254 nm and by gamma-detection with a scintillation detector GABI (Raytest).

### 2.2. Synthesis of reference compounds and precursors

#### 2.2.1. 3-(4-Fluorophenyl)-2-(4-methylsulfonylphenyl)-1*H*-indole **3**

The compound was prepared in a McMurry reaction with **4**, TiCl<sub>4</sub> and Zn as previously described in 62% yield.<sup>13</sup> mp: 234–236 °C, (lit.: 224–226 °C), <sup>1</sup>H NMR (400 MHz, DMSO-*d*<sub>6</sub>): δ 3.25 (s, 3H, SO<sub>2</sub>CH<sub>3</sub>); 7.08 (t, <sup>3</sup>*J* = 7.2 Hz, <sup>3</sup>*J* = 8.0 Hz, 1H, H<sub>indole</sub>); 7.22 (t, <sup>3</sup>*J* = 7.2 Hz, <sup>2</sup>*J* = 8.0 Hz, 1H, H<sub>indole</sub>); 7.28 (t, <sup>3</sup>*J* = 8.9 Hz, 2H, H<sub>F-phenyl</sub>); 7.38 (dd, <sup>3</sup>*J* = 8.7 Hz, <sup>4</sup>*J* = 5.7 Hz, 2H, H<sub>F-phenyl</sub>); 7.45 (d, <sup>3</sup>*J* = 8.0 Hz, 1H, H<sub>indole</sub>); 7.49 (d, <sup>3</sup>*J* = 8.0 Hz, 1H, H<sub>indole</sub>); 7.66 (d, <sup>3</sup>*J* = 8.5 Hz, 2H, H<sub>phenyl</sub>); 7.91 (d, <sup>3</sup>*J* = 8.5 Hz, 2H, H<sub>phenyl</sub>); 11.79 (s, 1H, NH) ppm; <sup>19</sup>F NMR (376 MHz, DMSO-*d*<sub>6</sub>): −116.32 ppm; ESI-MS (ES<sup>+</sup>): *m/z* = 388 (M+Na).

#### 2.2.2. 2-*N*(4-Methylsulfonylbenzoyl)-amino-4'-fluoro-benzophenone **4**

To a solution of 600 mg (2.79 mmol) 2-amino-4'-fluoro-benzophenone<sup>13</sup> and 446 μL triethylamine in 5.6 mL of dry THF was added a suspension of 609 mg (2.79 mmol) 4-(methylsulfonyl)benzoyl-chloride<sup>15</sup> suspended in 2.8 mL of THF with stirring under a nitrogen atmosphere. After 2 h at room temperature the mixture

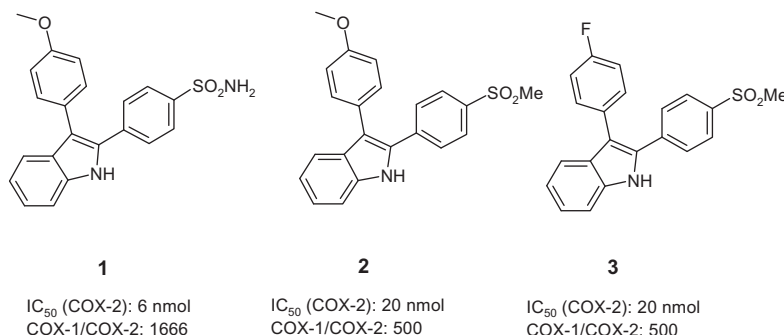


Figure 1. 2,3-Diarylsubstituted indoles as COX-2 inhibitors.<sup>13</sup>

was filtrated and evaporated to dryness. The residue was suspended in 15 mL of ethanol, the precipitate filtered off, washed with 5 mL of hot ethanol and 12 mL of water and purified by column chromatography (ethyl acetate/petroleum ether = 50:50) to give compound **4** (663 mg, 60%) as a colorless solid, mp 207–209 °C. <sup>1</sup>H NMR (400 MHz, DMSO-*d*<sub>6</sub>): δ 3.26 (s, 3H, SO<sub>2</sub>CH<sub>3</sub>); 7.30 (t, <sup>3</sup>J = 8.8 Hz, 2H, H<sub>F-phenyl</sub>); 7.36–7.39 (m, 1H, H<sub>ar</sub>); 7.49 (d, <sup>3</sup>J = 8.3 Hz, 1H, H<sub>ar</sub>); 7.66–7.68 (m, 2H, 2H<sub>ar</sub>); 7.76 (dd, <sup>3</sup>J = 8.8 Hz, <sup>4</sup>J = 5.6 Hz, 2H, H<sub>F-phenyl</sub>); 7.88 (d, <sup>3</sup>J = 8.5 Hz, 2H, H<sub>phenyl</sub>); 8.01 (d, <sup>3</sup>J = 8.5 Hz, 2H, H<sub>phenyl</sub>); 10.80 (br s, 1H, NH) ppm; ESI-MS (ES<sup>+</sup>): *m/z* = 420 (M+Na).

### 2.2.3. 2-(4-Methylphenylsulfonamido)-4'-(*N,N*-dimethylamino)-benzophenone **6**

In a heat dried flask was added 308 mg (2.3 mmol) of water free AlCl<sub>3</sub> and 600 mg (1.93 mmol) of 2-(4-methylphenylsulfonamido)-benzoyl chloride<sup>16</sup> **5** in portions under stirring to 10 mL of *N,N*-dimethylaniline at 0–5 °C. The mixture was kept at this temperature for 5 h and let come to room temperature overnight. After quenching with 100 mL of ice water, the solution was acidified with 1 M HCl to pH 2–3 and extracted with 3 portions of 50 mL ethyl acetate. The organic layer was washed with water until pH 5, dried with Na<sub>2</sub>SO<sub>4</sub> and evaporated. The excess of *N,N*-dimethylaniline was removed in high vacuum. The remaining solid was dissolved in ethyl acetate and by addition of petroleum ether a yellow product was precipitated. The precipitate was filtered off, dried and purified by column chromatography (ethyl acetate/petroleum ether = 40:60) to give compound **6** (297 mg, 38%) as a yellow solid, mp 171–175 °C. <sup>1</sup>H NMR (400 MHz, CDCl<sub>3</sub>): δ 2.17 (s, 3H, CH<sub>3</sub>); 3.09 (s, 6H, N(CH<sub>3</sub>)<sub>2</sub>); 6.56 (d, <sup>3</sup>J = 9.0 Hz, 2H, H<sub>phenyl</sub>); 6.94 (d, <sup>3</sup>J = 8.4 Hz, 2H, H<sub>phenyl</sub>); 7.10 (dd, <sup>3</sup>J = 7.6 Hz, 1H, H<sub>ar</sub>); 7.34–7.38 (m, 3H, 2H<sub>phenyl</sub>, H<sub>ar</sub>); 7.46 (d, <sup>3</sup>J = 7.0 Hz, 1H, H<sub>ar</sub>); 7.49 (d, <sup>3</sup>J = 8.3 Hz, 2H, H<sub>phenyl</sub>); 7.75 (d, <sup>3</sup>J = 8.3 Hz, 1H, H<sub>ar</sub>); 9.53 (br s, 1H, NH) ppm; <sup>13</sup>C NMR (101 MHz, CDCl<sub>3</sub>): δ 21.5; 40.2; 110.3; 123.7; 124.2; 124.5; 127.3; 129.0; 129.6; 131.8; 132.3; 133.0; 135.9; 137.9; 143.4; 153.7; 195.3 ppm; ESI-MS (ES<sup>+</sup>): *m/z* = 417 (M+Na).

### 2.2.4. 2-Amino-4'-(*N,N*-dimethylamino)-benzophenone **7**

A mixture of 1.3 g (3.3 mmol) **6** in 7.0 mL perchloric acid and 3.0 mL acidic acid was heated at a temperature of 100 °C with stirring for 3 h. The solution was hydrolyzed by careful addition to 150 mL of ice and water. After filtration the acidic mixture was alkalinized to neutral pH by addition of 25% aqueous NH<sub>3</sub>-solution, the yellow precipitate was collected and dried under vacuum. Purification occurred by dissolution at ethyl acetate, filtration via a small silica gel column and evaporation of the solvent to give compound **7** (400 mg, 59%) as a yellow solid, mp 118–123 °C. <sup>1</sup>H NMR (400 MHz, CDCl<sub>3</sub>): δ 3.06 (s, 6H, N(CH<sub>3</sub>)<sub>2</sub>); 5.63 (br s, 2H, NH<sub>2</sub>); 6.64–6.75 (m, 4H, 2H<sub>phenyl</sub>, 2H<sub>ar</sub>); 7.22–7.30 (m, 1H, H<sub>ar</sub>); 7.48 (d, <sup>3</sup>J = 6.4 Hz, 1H, H<sub>ar</sub>); 7.71 (d, <sup>3</sup>J = 8.6 Hz, 2H, H<sub>phenyl</sub>) ppm; <sup>13</sup>C NMR (101 MHz, CDCl<sub>3</sub>): δ 40.2; 110.6; 115.7; 116.9; 120.5; 126.7; 132.3; 132.9; 133.5; 149.7; 152.9; 197.2 ppm; ESI-MS (ES<sup>+</sup>): *m/z* = 263 (M+Na).

### 2.2.5. 2-*N*(4-Methylsulfonylbenzoyl)-amino-4'-(*N,N*-dimethylamino)-benzophenone **8**

To 350 mg (1.46 mmol) of **7** dissolved at 1.7 mL of dry THF under a nitrogen atmosphere was added 220 μL (1.6 mmol) of triethylamine and 320 mg (1.46 mmol) of 4-(methylsulfonyl)benzoyl-chloride<sup>15</sup> suspended in 1.3 mL of THF. After stirring for 2 h at room temperature, the suspension was filtrated and the residue washed with 3 portions of THF. The collected filtrates were evaporated and the residue purified by column chromatography (ethyl acetate/petroleum ether = 50:50) to give compound **8** (557 mg, 90%) as a yellow solid, mp 188–192 °C. <sup>1</sup>H NMR (400 MHz, CDCl<sub>3</sub>):

δ 3.08 (s, 3H, SO<sub>2</sub>CH<sub>3</sub>); 3.09 (s, 6H, N(CH<sub>3</sub>)<sub>2</sub>); 6.68 (d, <sup>3</sup>J = 9.1 Hz, 2H, H<sub>phenyl</sub>); 7.18 (dd, <sup>3</sup>J = 7.6 Hz, 1H, H<sub>ar</sub>); 7.60 (dd, <sup>3</sup>J = 7.8 Hz, 1H, H<sub>ar</sub>); 7.67 (d, <sup>3</sup>J = 7.8 Hz, <sup>4</sup>J = 1.4 Hz, 1H, H<sub>ar</sub>); 7.74 (d, <sup>3</sup>J = 9.1 Hz, 2H, H<sub>phenyl</sub>); 8.07 (d, <sup>3</sup>J = 8.5 Hz, 2H, H<sub>phenyl</sub>); 8.20 (d, <sup>3</sup>J = 8.5 Hz, 2H, H<sub>phenyl</sub>); 8.73 (d, <sup>3</sup>J = 8.4 Hz; 1H, H<sub>ar</sub>); 11.78 (br s, 1H, NH); <sup>13</sup>C NMR (101 MHz, CDCl<sub>3</sub>): δ 40.2; 44.6; 110.7; 121.6; 122.9; 125.2; 125.3; 128.1; 128.5; 133.0; 133.2; 139.5; 139.9; 143.3; 153.7; 163.9; 197.5 ppm; ESI-MS (ES<sup>+</sup>): *m/z* = 445 (M+Na).

### 2.2.6. 2-*N*(4-Methylsulfonylbenzoyl)-amino-4'-(*N,N,N*-trimethylammonium)-benzophenone trifluoromethanesulfonate **9**

In 10 mL of nitromethane was dissolved 250 mg (0.59 mmol) of **8** under stirring and 88 μL (0.8 mmol) of methyl-trifluoromethanesulfonate was added. After 12 h at room temperature the nitromethane was evaporated in vacuum and the residue dissolved at 1 mL of dichloromethane. The solution was refrigerated overnight; the precipitate was filtered off, washed with water free methanol and dried under vacuum to give compound **9** (159 mg, 46%) as a light yellow solid, mp 162–165 °C. <sup>1</sup>H NMR (400 MHz, DMSO-*d*<sub>6</sub>): δ 3.26 (s, 3H, SO<sub>2</sub>CH<sub>3</sub>); 3.59 (s, 9H, N(CH<sub>3</sub>)<sub>3</sub>); 7.31 (dt, <sup>3</sup>J = 7.6 Hz, <sup>4</sup>J = 1.4 Hz, 1H, H<sub>ar</sub>); 7.47 (d, <sup>3</sup>J = 7.8 Hz, <sup>4</sup>J = 1.4 Hz, 1H, H<sub>ar</sub>); 7.65 (dd, <sup>3</sup>J = 8.0 Hz, <sup>4</sup>J = 1.0 Hz, 1H, H<sub>ar</sub>); 7.89 (dt, <sup>3</sup>J = 7.6 Hz, <sup>4</sup>J = 1.4 Hz, 1H, H<sub>ar</sub>); 7.92–7.96 (m, 4H, H<sub>phenyl</sub>); 8.03 (d, <sup>3</sup>J = 8.6 Hz, 2H, H<sub>phenyl</sub>); 8.06 (d, <sup>3</sup>J = 9.1 Hz, 2H, H<sub>phenyl</sub>); 10.90 (br s, 1H, NH); <sup>19</sup>F NMR (376 MHz, DMSO-*d*<sub>6</sub>): –78.18 ppm; <sup>13</sup>C NMR (101 MHz, DMSO-*d*<sub>6</sub>): δ 43.2; 56.4; 120.6; 124.6; 125.2; 127.1; 128.3; 129.9; 131.0; 131.0; 132.5; 136.0; 138.3; 138.4; 143.4; 149.6; 164.3; 193.4 ppm; ESI-MS (ES<sup>+</sup>): *m/z* = 437 (M<sup>+</sup>), (M = 437.53 calcd for C<sub>24</sub>H<sub>25</sub>N<sub>2</sub>O<sub>4</sub>S).

### 2.3. Radiosynthesis of 3-(4-[<sup>18</sup>F]fluorophenyl)-2-(4-methylsulfonylphenyl)-1*H*-indole [<sup>18</sup>F]-**3** via McMurry cyclization

Synthesis of [<sup>18</sup>F]-**3** was performed using an automated synthesizer module in a two-step procedure; firstly by reacting [<sup>18</sup>F]fluoride with the trimethylammonium precursor **9** forming the intermediate [<sup>18</sup>F]-**4** and secondly by McMurry cyclization with titanium tetrachloride and zinc. Briefly 15 mg of **9** dissolved at 2.5 mL of acetonitrile were heated with about 8 GBq of the dried [<sup>18</sup>F]KF/K<sub>222</sub> complex at 110 °C for 15 min. After cooling to 60 °C the acetonitrile was removed in a stream of nitrogen and a freshly prepared suspension of 20 mg zinc in 2.5 mL dry THF containing 37 μL of TiCl<sub>4</sub> was added. The temperature was maintained at 90 °C for 15 min to perform the McMurry cyclization and the THF was once more removed under a nitrogen stream at 70 °C. The residue was diluted with 3 mL of eluent, passed through a cartridge filled with sea sand to remove insoluble material and conducted to semi-preparative HPLC using an isocratic eluent (acetonitrile/water = 70:30). The radiotracer [<sup>18</sup>F]-**3** was eluted at 8–9 min at a flow rate of 4 mL/min. The product was separated from the eluent by means of solid phase extraction (Lichrolut RP18, 500 mg, Merck), eluted from the cartridge with 0.7 mL of ethanol and reconstituted for biological investigation with 6.5 mL of 0.9% sodium chloride solution. In this way [<sup>18</sup>F]-**3** was synthesized in 80 min synthesis time in 10% total decay corrected yield from [<sup>18</sup>F]fluoride in radiochemical purity >98% and a specific activity of 74–91 GBq/μmol at the end of synthesis (EOS).

## 2.4. Radiopharmacological characterization

### 2.4.1. Cell uptake studies in vitro

Uptake experiments for evaluation of compound [<sup>18</sup>F]-**3** in vitro were performed in various cell models following the protocol published elsewhere with some modifications.<sup>12</sup> Therefore, THP-1 (human monocyte/macrophage line; DSMZ ACC 16), FaDu (human squamous cell carcinoma line; ATCC HTB-43), HT-29 (human

colorectal adenocarcinoma line; ATCC HTB-38), A2058 (human malignant melanoma line; ATCC CRL-11147) and A375 (human malignant melanoma line; ATCC CRL-1619) were used. Cells were routinely cultivated in RPMI 1640 medium (THP-1, FaDu), McCoy's 5A medium (HT-29), or Dulbecco's modified Eagle's medium (A2058, A375) supplemented with 10% (v/v) heat-inactivated fetal calf serum (FCS), penicillin (100 U/mL), streptomycin (100 µg/mL), and glutamine (4 mM) at 37 °C and 5% CO<sub>2</sub> in a humidified incubator. Cells were passaged twice a week by mild enzymatic dissociation using 0.25% trypsin/EDTA. Pro-inflammatory stimulation (differentiation to macrophages) of THP-1 cells was performed by adding 64 nM phorbol myristate acetate (TPA) for 72 h. Radiotracer uptake studies were performed in (a) monolayer cultures (FaDu, HT-29, A2058, A375, TPA-stimulated THP-1), (b) in suspension cells (unstimulated THP-1), and (c) in multicellular spheroids (HT-29). The pre-analytical conditions were as follows: (a) cells were seeded in 24-well plates at a density of  $5 \times 10^4$  cells/mL and grown to confluence, (b) cells were centrifuged and resuspended in fresh RPMI medium containing 10% FCS in 24-well plates at a density of  $5 \times 10^5$  cells/mL, and (c)  $1 \times 10^4$  cells per well were seeded in non-adherent round-bottom 96-well plates in the presence of 0.24% (w/v) methylcellulose and were allowed to form a single spheroid per well for 3 d without medium exchange and, after 80% of the medium was renewed, for additional 4 d (total volume per well was 100 µL). Spheroid diameters were measured using an inverse microscope equipped with a guidable desk and digital camera shortly before the addition of radiotracers. In this study only spheroids with a diameter of  $300 \pm 10$  µm (3 d) and  $600 \pm 10$  µm (7 d) were used. The cell tracer uptake experiments using compound [<sup>18</sup>F]-**3** (0.4 MBq/mL; specific activity at application time, 74 GBq/µmol) were performed in quadruplicate in medium at 37 °C for 30, 60, and 120 min. For blocking experiments, the cells were preincubated for 30 min with the corresponding non-radioactive reference compound **3** (100 µM). To investigate the effect of the P-glycoprotein efflux pump pretreatment of cells with cyclosporine A (100 µM) and verapamil (100 µM), respectively was performed for 60 min. In order to characterize normoxia in the HT-29 monolayers and intrinsic hypoxia in HT-29 spheroids also uptake experiments with 0.4 MBq <sup>18</sup>F-labeled fluoromisonidazole ([<sup>18</sup>F]FMISO; specific activity at application time, 115 GBq/µmol; incubation time 4 h) were performed. Therefore, [<sup>18</sup>F]FMISO was prepared via one pot, two-step synthesis procedure by use of a modified Tracerlab<sub>FXN</sub> synthesis module (GE).<sup>17</sup> After the tracer uptake was stopped with 1 mL ice-cold PBS, the monolayer and suspension cells were washed three times with PBS and dissolved in 0.5 mL NaOH (0.1 M containing 1% (w/v) sodium dodecylsulfate). The radioactivity in cell extracts was then measured with a Cobra II gamma counter (Canberra-Packard, Meriden, CT, USA). Spheroids were harvested and washed five times with PBS on filters using a commercial cell harvester (Filtermate 196, Canberra-Packard, Meriden, CT, USA). The filters were then transferred into tubes containing 350 µL distilled water and radiotracer uptake was measured with a Cobra II gamma counter. Total protein concentration in cell extracts was determined by the bicinchoninic acid assay (BCA; Pierce, Rockford, Ill, USA) using bovine serum albumin as protein standard. For determination of mean protein concentration in spheroids additional 96-well plates were prepared in parallel. Subsequently, 8 spheroids of each target diameter were pooled in quintuplicate, disintegrated in 0.5 mL NaOH (0.1 M containing 1% (w/v) sodium dodecylsulfate and measured using BCA method. Uptake data for all experiments are expressed as percent of injected dose per µg protein (%ID/µg protein).

#### 2.4.2. Western blot analysis

In order to characterize protein expression of COX-1 and COX-2 in the models used, cells were analyzed by Western blotting.

Therefore, cells were washed with ice-cold PBS and lysed in lysis buffer (50 mM Tris-HCl pH 7.5, 150 mM NaCl, 2% Nonidet P40, 0.1% SDS with 1 mM sodium orthovanadate, 1 mM NaF, 10 mM β-glycerophosphate, 1 mM dithiothreitol (DTT), 1 mM phenylmethyl sulfonyl fluoride, and 1 µg/mL leupeptine). Cells were centrifuged at  $15,000 \times g$  for 15 min at 4 °C. Then 50 µg of protein were mixed with sample buffer, denatured at 99 °C for 15 min and separated on 7.5% SDS-polyacrylamide gels. Proteins were transferred to nitrocellulose membranes by electroblotting and blocked for 1 h at room temperature in TBS/Tween (50 mM Tris-HCl pH 8.0, 150 mM NaCl, 0.05% Tween-20) containing 5% skimmed milk powder. Membranes were incubated with the primary antibodies for COX-1 (C-20, sc-1752) or COX-2 (M-19, sc-1747) (both 1:500, Santa Cruz Biotechnology) at 4 °C overnight, followed by incubation with secondary peroxidase-conjugated anti-goat IgG antibodies (1:10,000, A5420, Sigma-Aldrich) for 1 h at room temperature. After washing with TBS/Tween proteins were visualized by chemiluminescence using the SuperSignal West Pico Chemiluminescent Substrate (Pierce, Rockford, USA) and the MF ChemiBIS bioimager (Biostep). For detection of β-actin primary polyclonal antibody β-actin IgG (1:1000, A5060, Sigma-Aldrich) and secondary peroxidase-conjugated antibody anti-rabbit IgG (1:10,000, A0545, Sigma-Aldrich) were used.

#### 2.4.3. Inhibition of COX-2 activity

The influence of the corresponding nonradioactive reference compound **3** on prostaglandin E<sub>2</sub> (PGE<sub>2</sub>) synthesis and thus interaction with cyclooxygenases was characterized in supernatants of HT-29, FaDu, and A375 cells by liquid chromatography-tandem mass spectrometry (LC-MS/MS) according to Cao et al.<sup>18</sup> with some modifications. Therefore, cells were seeded in 12-well plates ( $2.5 \times 10^6$  cells/well) and grown for 24 h. The medium was changed and the three tumor cell lines were incubated with fresh medium containing either 1 or 10 µM of compound **3** for 25 h. Then to aliquots of cell culture supernatants (1 mL) were added the deuterated internal standard d<sub>4</sub>-PGE<sub>2</sub> (0.7 nM; Cayman Chemical, Ann Arbor, MI, USA) and, as preservatives, citric acid (72 mM) and butylated hydroxytoluene (BHT, 3.2 mM). The samples were acidified with glacial acetic acid to pH 4.0, shock frozen with liquid nitrogen, and stored at -65 °C. For analysis, samples were thawed and immediately extracted three times with 1 mL of diethyl ether under a nitrogen atmosphere to prevent oxidation. The organic layers were combined and the solvent was evaporated under a gentle stream of nitrogen at room temperature. The resulting residue was reconstituted in 100 µL of mobile phase (composition at starting point) for the chromatographic separation. Analyses were carried out on an Agilent 1100 HPLC system (Agilent Technologies, Santa Clara, CA, US) coupled to a Micromass Quattro LC mass spectrometer (Micromass, Manchester, UK). Therefore, sample aliquots of 15 µL were injected onto a Hypercarb<sup>®</sup> column (100 × 2.1 mm, 5 µm; Thermo Fisher Scientific, Waltham, MA, US) and chromatographed at 35 °C using an eluent comprising of mobile phase A (10 mM NH<sub>4</sub>Ac, pH 10.5) and mobile phase B (methanol/acetone-trile 60/40, v/v) at a flow rate of 150 µL/min. The gradient was as follows: %A; held 95% for 10 min, decreased to 5% in 15 min, held 5% for 20 min, decreased to 1% in 0.5 min, held 1% for 5 min, increased to 95% in 5 min. Electrospray mass spectrometry was performed in the negative ion mode due to the acidic character of the investigated eicosanoids using selected reaction monitoring (SRM). The electrospray capillary voltage and the source temperature were set at 4 kV and 100 °C. Desolvation gas (nitrogen) temperature was 150 °C. The specific mass transitions (quantitation transition; Cone -18 V, E<sub>coll</sub> 12 V) used for PGE<sub>2</sub> determination ([M-H]<sup>-</sup>; PGE<sub>2</sub> m/z 351; PGE<sub>2</sub>-d<sub>4</sub>, m/z 355) were PGE<sub>2</sub> m/z 351 → m/z 333 and PGE<sub>2</sub>-d<sub>4</sub> m/z 355 → m/z 337 corresponding to the [M-H-H<sub>2</sub>O]<sup>-</sup> ions. A dwell time of 600 ms was applied to monitor the

two SRM transitions. Calibration curves were obtained by plotting the peak area ratio for PGE<sub>2</sub>-d<sub>4</sub>-PGE<sub>2</sub> ion pair versus the mass ratio of the analytes and the internal standard, respectively. Calibration curves were analyzed by unweighted least-squares linear regression analysis and were found to be linear over the range studied (0.03–1000 nM;  $R^2 > 0.996$ ). The limit of determination of this approach was ascertained at 15 pM (220 fmol/injection).

Moreover, the ability of the corresponding nonradioactive reference compound **3** to inhibit ovine COX-1 and recombinant human COX-2 was determined using an enzymatic fluorescence-based cyclooxygenase inhibitor assay (catalog number 700100, Cayman Chemical, Ann Arbor, MI, USA) according to the manufacturer's protocol. The potent and selective COX-2 inhibitor celecoxib was used as reference compound. The COX inhibitors were assayed in concentrations ranging from 10<sup>-10</sup> M to 10<sup>-3</sup> M. PRISM5 software was used for the calculation of the IC<sub>50</sub> values.

#### 2.4.4. Stability studies in vitro and in vivo

**2.4.4.1. In vitro.** The stability of radiotracer [<sup>18</sup>F]-**3** in vitro after incubation with both rat whole blood and plasma was evaluated by radio-HPLC. Therefore, 0.5 MBq of radiotracer were added to 400 µL of blood sample taken from male Wistar-Unilever rats (strain HsdCpb:WU, Harlan Winkelmann, Borcheln, Germany) and incubated in a thermo-mixer at 37 °C at 600 rpm for 5, 30 and 60 min. Plasma was separated by centrifugation (3 min, 13,000 × g) followed by precipitation of plasma proteins with acetonitrile/water/trifluoroacetic acid (50:45:5) in a 1:2 ratio. The clear supernatant separated by second centrifugation (3 min, 13,000 × g) was used for analysis. For evaluation of in vitro stability in rat plasma the blood cells have been removed by centrifugation before addition of the radiotracer.

**2.4.4.2. In vivo.** Male Wistar-Unilever rats ( $n = 2$ ; body weight 150 ± 12 g) were anesthetized with desflurane (9–10% v/v, 30% oxygen/air). The threshold value for breathing frequency was 65 breaths/min. Animals were put in supine position and placed on a heating pad to maintain body temperature. The spontaneously breathing rats were heparinized with 100 units/kg heparin (Heparin-Natrium 25.000-ratiopharm®, ratiopharm GmbH, Germany) by subcutaneous injection to prevent blood clotting on intravascular catheters. After local anesthesia with lignocain (1%; Xylocitin® loc, mibe, Jena, Germany) into the right groin, a catheter (0.8 mm Umbilical Vessel Catheter, Tyco Healthcare, Tullamore, Ireland) was introduced into the right femoral artery for arterial blood sampling. A second needle catheter (35 G) was placed into a tail vein and was used for [<sup>18</sup>F]-**3** radiotracer injection (30 MBq in 0.5 mL of E153/10% ethanol, infusion 1 mL/min). Arterial blood samples were taken 1, 3, 5, 10, 20, 30 and 60 min after injection. Arterial plasma was separated by centrifugation followed by precipitation and removal of plasma proteins as described above. The radio-HPLC system (Agilent 1100 series) applied for metabolite analysis was equipped with UV detection (254 nm) and an external radiochemical detector (RAMONA, Raytest GmbH, Straubenhardt, Germany). Analysis was performed on a Zorbax C18 300SB (250 × 9.4 mm; 4 µm) column with an eluent system C (water + 0.1%TFA) and D (acetonitrile + 0.1% TFA) in a gradient 5 min 95% C, 10 min to 95% D and 5 min at 95% D at a flow rate of 3 mL/min. All animal procedures and experiments were carried out according to the guidelines of the German Regulations for Animal Welfare. The protocols were approved by the local Ethical Committee for Animal Experiments.

#### 2.4.5. Small animal PET studies in vivo

Dynamic small animal PET studies for evaluation of compound [<sup>18</sup>F]-**3** in vivo were performed in HT-29 tumor-bearing mice. Therefore, NMRI *nu/nu* mice (Technische Universität Dresden,

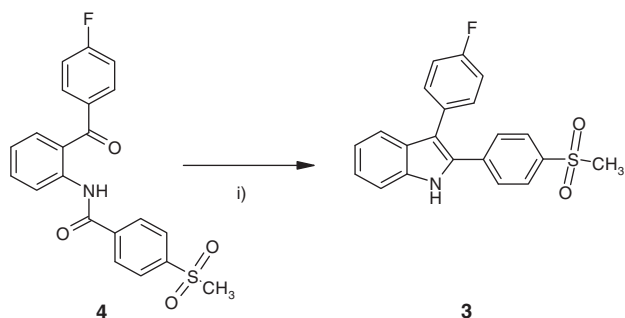
Experimentelles Zentrum der Medizinischen Fakultät Carl Gustav Carus, Dresden, Germany) were subcutaneously xenotransplanted into the right hind leg with human colorectal adenocarcinoma HT-29 according to a protocol published elsewhere.<sup>19</sup> When tumor size reached a diameter of about of 7–9 mm, imaging studies were performed. General anesthesia of HT-29 tumor-bearing mice ( $n = 8$ , body weight 40 ± 3 g) was induced and maintained with inhalation of 10% desflurane in 30% oxygen/air. Mice were positioned and immobilized prone with their medial axis parallel to the axial axis of the scanner (microPET® P4, Siemens preclinical solutions, Knoxville, TN, USA). In the PET experiments, 20 MBq of [<sup>18</sup>F]-**3** (in 0.5 mL of E153/10% ethanol) was administered intravenously as an infusion (1 mL/min) with a syringe pump (Harvard Apparatus, Holliston, Ma, USA) using a needle catheter into a tail vein. A transmission scan was carried out prior to the injection of [<sup>18</sup>F]-**3** using a rotating <sup>57</sup>Co point source. PET acquisition was started with a delay of 30 s after beginning of the radiotracer infusion. Emission data were collected continuously for 120 min after injection of [<sup>18</sup>F]-**3**. The 3D list mode data were sorted into sinograms with 38 frames (15 × 10 s, 5 × 30 s, 5 × 60 s, 4 × 300s, 9 × 600s). The data were decay, scatter and attenuation corrected. The data were normalized to the injected radioactivity by using <sup>18</sup>F-standards from the injection solution measured in a  $\gamma$ -well counter (Isomed 2000, Germany) cross calibrated to the PET scanner and expressed in percent of injected dose per cubic centimeter (%ID/cm<sup>3</sup>). The frames were reconstructed by Ordered Subset Expectation Maximization applied to 3D sinograms (OSEM3D) with 14 subsets, 15 OSEM3D iterations, 25 maximum a posteriori (MAP) iterations, and 1.8 mm resolution using the FastMAP algorithm (Siemens Preclinical Solutions, Knoxville, TN). The pixel size was 0.07 by 0.07 by 0.12 cm, and the spatial resolution in the center of field of view was 1.8 mm. No correction for partial volume effects was applied. The image volume data were converted to Siemens ECAT7 format further processed using the ROVER software (ABX GmbH, Radeberg, Germany). Masks for defining three-dimensional regions of interest (ROI) were set with ROI's defined by thresholding and ROI time activity curves (TAC) were derived for the subsequent data analysis. The standardized uptake values (SUV<sub>PET</sub>) were calculated over the ROI as the ratio of activity concentration at time *t* and injected dose at the time of injection divided by body weight.

### 3. Results and discussion

#### 3.1. Synthesis of labeling precursors and reference compounds

Our primary synthetic efforts were directed on the synthesis of the nonradioactive reference compound 3-(4-fluorophenyl)-2-(4-methylsulfonylphenyl)-1H-indole **3**. The synthesis sequence started from 2-amino-benzoic acid, the amino group was protected by tosylation, followed by a Friedel–Crafts acylation with fluorobenzene. After deprotection the amino function was reacted with 4-methylsulfonyl-benzoic acid chloride to give the key intermediate 2-N(4-methylsulfonylbenzoyl)-amino-4'-fluoro-benzophenone **4**. The final step was the cyclization of **4** with low-valent titanium and zinc in THF to form the indole skeleton by the McMurry cyclization (Scheme 1).<sup>20</sup>

Introduction of fluorine-18 onto the aromatic system is generally realized by nucleophilic substitution of a suitable leaving group, preferred a trimethylamino- or nitro- functionality with [<sup>18</sup>F]fluoride. Due to the weak nucleophilic properties of the anionic [<sup>18</sup>F]fluoride, an activation of the aromatic system by strong electron withdrawing groups such as nitrile and carbonyl group is essential for facilitating and accelerating the reaction. In the present case of a diarylsubstituted indole a direct nucleophilic attack with [<sup>18</sup>F]fluoride appeared to be not very promising. Considering this we decided to develop a precursor molecule having an



**Scheme 1.** Synthesis of reference compound **3** via McMurry cyclization. Reagents: (i)  $\text{TiCl}_4$ , Zn, THF.

electron withdrawing carbonyl group in *para*-position to the leaving group for introduction of the  $^{18}\text{F}$  radiolabel and to perform the McMurry cyclization as the second step. This radiolabeling approach including a McMurry reaction has to the best of our knowledge not been practiced so far. A detailed look in the literature revealed that the required dimethylamino-substituted benzophenones from type of **8** or **9** are still unknown, what pushed us to set up a new synthetic route (Scheme 2).

In the literature Hu et al.<sup>13</sup> described the formation of disubstituted benzophenones as multi-step procedure comprising the reaction of tosylated anthranilic acid with  $\text{PCl}_5$  followed by a Friedel–Crafts acylation with the second aromatic moiety without work-up of the acid chloride **5**. By application of this protocol with *N,N*-dimethylaniline as aromatic partner at temperatures between 50 °C and 80 °C, we always obtained deep blue colored mixtures, that were supposed to be derivatives of the triphenylmethane dyes like Michler's ketone.

In a parallel approach we prepared the corresponding benzamide of anthranilic acid and performed the acylation with *N,N*-dimethylaniline with  $\text{POCl}_3$  at 150 °C under Vilsmeier–Haack conditions.<sup>21</sup> However the yield of 2-(4-methylphenylsulfonamido)-4'-(*N,N*-dimethylamino)-benzophenone **6** via this route was unsatisfying 17%.

Consequently we decided for two step approach; an isolation and purification of the 2-(4-methylphenylsulfonamido)-benzoyl chloride **5** as described in the literature<sup>16</sup> and to react **5** with *N,N*-dimethylaniline and  $\text{AlCl}_3$  under Friedel–Crafts conditions in a second step; in this way **6** was obtained with 38% yield.

The cleavage of the tosyl group from **6** in concentrated sulfuric acid at 120 °C according to Hu et al.<sup>13</sup> did neither yield the amine **7** in sufficient yield nor quality. From that reason we chose a deprotection method described by Kudav et al.<sup>22</sup> basing on a mixture of  $\text{HClO}_4/\text{CH}_3\text{COOH}$  at 100 °C, and were finally able to isolate the 2-amino-4'-(*N,N*-dimethylamino)-benzophenone **7** in 59% yield. Subsequently **7** was successfully coupled with 4-methylsul-

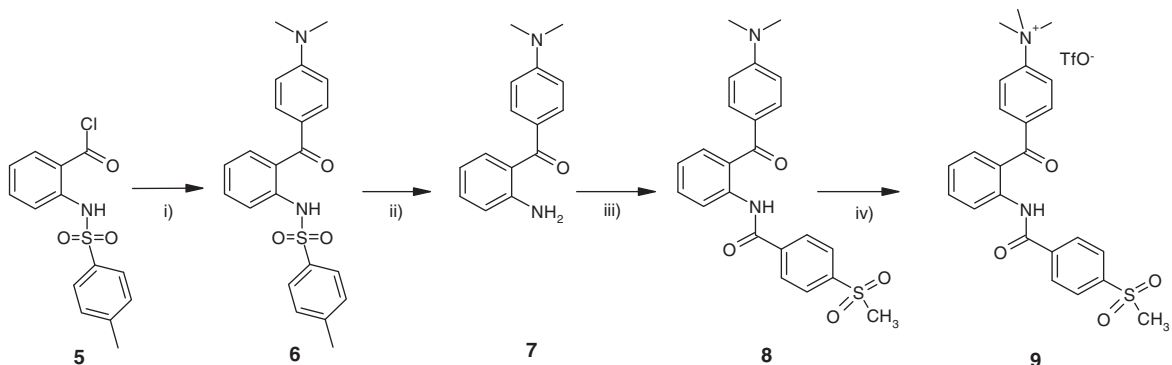
fonyl-benzoylchloride in THF to give 2-*N*-(4-methylsulfonylbenzoyl)-amino-4'-(*N,N*-dimethylamino)-benzophenone **8** in 90% yield. Ultimately the trimethyl ammonium salt **9** was obtained by reaction of **8** with methyl-trifluoromethanesulfonate in nitromethane as the desired precursor for radiofluorination.

### 3.2. Radiosynthesis of [ $^{18}\text{F}$ ]-**3** via McMurry cyclization

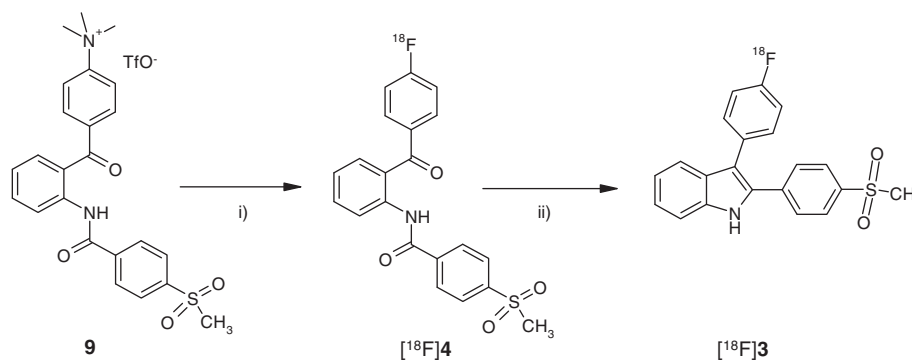
The approach to obtain the radiolabeled COX-2 inhibitor [ $^{18}\text{F}$ ]-**3** is outlined in Scheme 3. As mentioned above, the nucleophilic substitution with [ $^{18}\text{F}$ ]fluoride should be accomplished on precursor molecule **9** to take advantage of the electron withdrawing effect of the carbonyl group. The ring closure to the indole structure had to be performed subsequently via McMurry cyclization of the radiolabeled intermediate [ $^{18}\text{F}$ ]-**4** with zinc and titanium tetrachloride.

In a first number of experiments we investigated the optimal conditions for introduction of [ $^{18}\text{F}$ ]fluoride into precursor **9** with respect of solvent and temperature. Briefly 15 mg of precursor were heated with the dried [ $^{18}\text{F}$ ]KF/Kryptofix<sub>222</sub> complex in 1.5 mL of solvent for 15 min at temperature ranging between 90 and 140 °C. The reaction mixture was examined by analytical radio-HPLC for the amount of radiolabeled intermediate [ $^{18}\text{F}$ ]-**4** whereas the retention time of the UV-absorption from the nonradioactive compound **4** served as the reference. The results are summarized in Table 1, where it is recognizable that the ratio of [ $^{18}\text{F}$ ]-**4** increased with the temperature. By using DMF as the solvent and 140 °C reaction temperature 31% of [ $^{18}\text{F}$ ]fluoride could be introduced in **9** as a maximum yield (entries 1–5).

Beginning from entry 4 we tried to perform the McMurry cyclization by addition of a complex formed from zinc and  $\text{TiCl}_4$  in THF to the intermediate and by heating the mixture at 100 °C. At the first go a ratio of 12% of the final product [ $^{18}\text{F}$ ]-**3** was detected by radio-HPLC. However a second radiolabeled product was observed, what was supposed to be the free amino compound, formed by alkaline hydrolysis of the amide intermediate [ $^{18}\text{F}$ ]-**4** initiated from the basic [ $^{18}\text{F}$ ]KF/Kryptofix<sub>222</sub> conditions. To circumvent this situation we performed the radiolabeling under neutral pH conditions with a Kryptofix<sub>222</sub>/ $\text{C}_2\text{K}_2\text{O}_4$  complex.<sup>23</sup> Unfortunately the McMurry reaction was inhibited under these conditions giving only a low yield of [ $^{18}\text{F}$ ]-**3**; the reason for this behavior is the competitive complex formation of titanium and oxalate (entry 5). In all our attempts to replace the THF in the McMurry reaction by another solvent, we observed by radio-HPLC in majority of cases a good yield of the intermediate [ $^{18}\text{F}$ ]-**4** but only less or nothing of the desired final product [ $^{18}\text{F}$ ]-**3** (entries 4, 6, and 10). This is conform with findings in literature, describing that the low valent titanium reagent is only formed by support of by weak coordinating solvents like diethyl ether, THF or 1,2-dimethoxyethane (DME).<sup>20</sup> In entries 7–9 DMF was applied as the solvent for the first and THF as the



**Scheme 2.** Synthesis of labeling precursor **9**. Reagents: (i) *N,N*-dimethylaniline,  $\text{AlCl}_3$ ; (ii)  $\text{HClO}_4/\text{CH}_3\text{COOH}$ ; (iii)  $\text{CH}_3\text{SO}_2\text{C}_6\text{H}_4\text{COCl}$ , TEA, THF; (iv)  $\text{CF}_3\text{SO}_3\text{CH}_3$ , nitromethane.



**Scheme 3.** Radiosynthesis of [ $^{18}\text{F}$ ]-**3** via McMurry coupling. Reagents: (i) [ $^{18}\text{F}$ ]fluoride,  $\text{K}_{222}/\text{K}_2\text{CO}_3$ , DMF; (ii)  $\text{TiCl}_4$ , Zn, THF.

**Table 1**  
Yields and conditions of  $^{18}\text{F}$ -radiolabeling and McMurry reaction starting from precursor **9**, radiochemical yields (RCY) are estimated from the product ratio in radio-HPLC

	$^{18}\text{F}$ labeling conditions		RCY [ $^{18}\text{F}$ ]- <b>4</b> (%)	McMurry conditions		RCY [ $^{18}\text{F}$ ]- <b>3</b> (%)
	Solvent	Temperature ( $^{\circ}\text{C}$ )		Solvent	Temperature ( $^{\circ}\text{C}$ )	
1	$\text{CH}_3\text{CN}$	90	10	—	—	—
2	DMF	90	1	—	—	—
3	DMF	120	18	—	—	—
4	DMF	140	31	$\text{CH}_3\text{CN}/\text{THF}$	100	12
5	$\text{DMF}^a$	140	30	THF	100	4
6	DMF	140	26	$\text{CH}_3\text{CN}$	100	1
7	DMF	140	n.d.	THF	100	16
8	DMF	140	n.d.	$\text{THF}^b$	100	25
9	DMF	140	n.d.	THF	90	20
10	DMSO	140	44	DMSO/THF	100	0
11	$\text{CH}_3\text{CN}$	120	1	THF	100	57
12	$\text{CH}_3\text{CN}$	110	10	THF	90	50
13	$\text{CH}_3\text{CN}$	110	2	THF	90	82

n.d. not determined.

<sup>a</sup> Potassium oxalate/Kryptofix K222 complex.

<sup>b</sup> Double amount of  $\text{TiCl}_4$ .

solvent for the second step, but even with increasing amount of titanium tetrachloride and zinc the yield of [ $^{18}\text{F}$ ]-**3** did not exceed 25%. We suspected that the DMF still present in the second step so far, could act as an inhibitor of the McMurry cyclization. Reasoning we decided to perform the radiolabeling in acetonitrile at 110–120  $^{\circ}\text{C}$ , to remove the solvent in a stream of nitrogen under vacuum and to perform the McMurry reaction in pure THF. Under these conditions the amount of desired radiotracer [ $^{18}\text{F}$ ]-**3** was enhanced to 82% and the intermediate [ $^{18}\text{F}$ ]-**4** was more or less completely consumed (entries 11–13). Finally the reaction steps were transferred to an automated sequence on the synthesizer module, covering radiolabeling, McMurry cyclization, and purification on a semi-preparative column, solid phase extraction and formulation of the radiotracer [ $^{18}\text{F}$ ]-**3** for radio pharmacological investigation. It should be noted that prior semi-preparative HPLC the mixture was passed through a filter unit containing see sand to remove any insoluble material originated from titanium. A second evaporation step under vacuum was useful, because the injection of the THF raw product solution into the semi-preparative HPLC was responsible for a poor separation on the column. Whole process of automated radiosynthesis of [ $^{18}\text{F}$ ]-**3** is displayed in a flow diagram at Scheme 4. In this way starting from 8000 MBq of [ $^{18}\text{F}$ ]fluoride 400–500 MBq of [ $^{18}\text{F}$ ]-**3** was obtained in >98% radiochemical purity with a specific activity about 74–91 GBq/ $\mu\text{mol}$  (EOB) after 80 min total synthesis time.

### 3.3. Distribution coefficient

The octanol/buffer distribution coefficient ( $\log D_{\text{Oct}7.4}$ ) at pH 7.4 was measured using radiolabeled [ $^{18}\text{F}$ ]-**3** in phosphate buffer

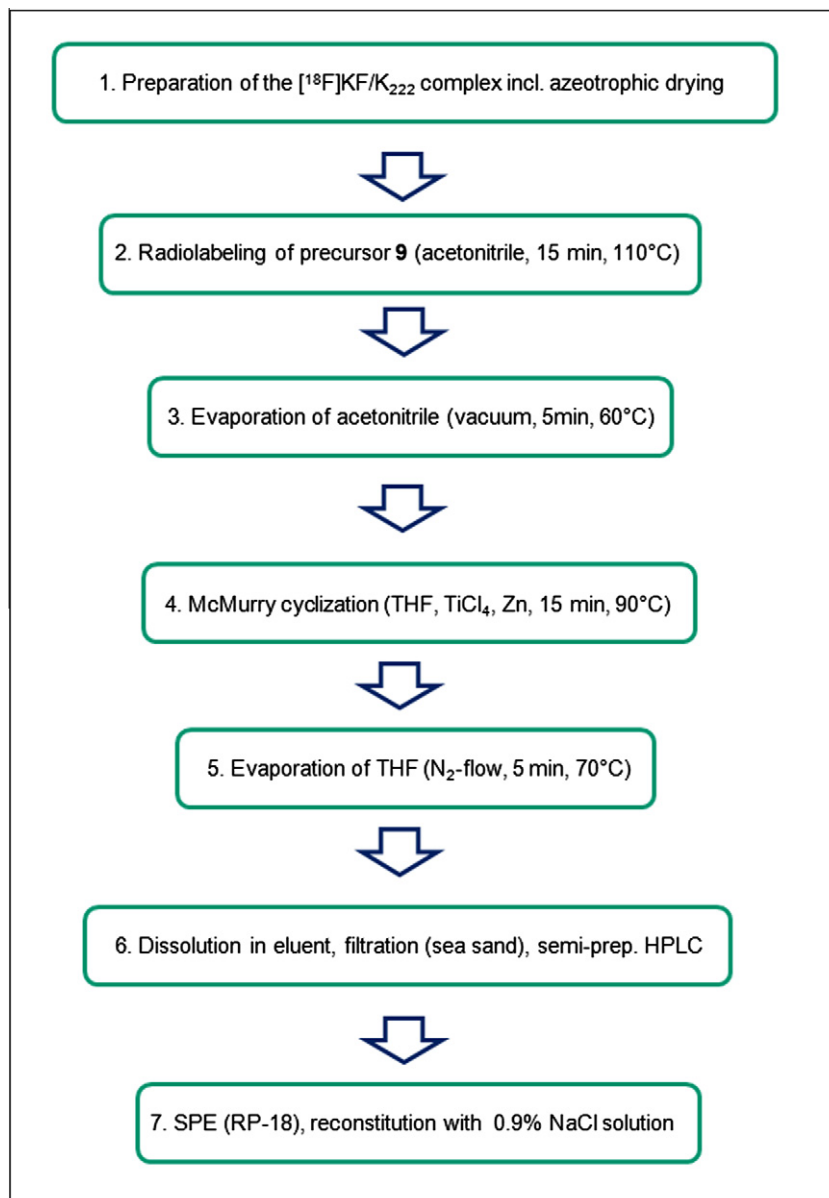
(0.1 M) and an equal volume of water-saturated *n*-octanol in a separation funnel. After vortexing for 1 min, the mixture was fixed, and the two phases were allowed to separate. Aliquots of the separated phases were assayed for tracer activity concentration by the gamma well counter. Samples were analyzed in fivefold and re-extracted three times to ensure stability of the  $\log D_{\text{Oct}7.4}$  value. In this way the  $\log D_{\text{Oct}7.4}$  of [ $^{18}\text{F}$ ]-**3** was determined to be  $1.2 \pm 0.2$ .

### 3.4. Cell uptake studies in vitro

Cellular expression of COX proteins was detected after SDS-PAGE by Western blotting using specific antibodies for COX-1 (68 kDa) and COX-2 (70 kDa). As internal control also  $\beta$ -actin (42 kDa) was analyzed. Multiple protein bands in the COX-1 lane between 60 kDa and 75 kDa result from different glycosylated or splicing variants of COX-1 (Fig. 2).<sup>24,25</sup>

Different human tumor cell lines were used to study the uptake of compound [ $^{18}\text{F}$ ]-**3** in vitro. All cell lines used show a weak constitutive expression of COX-1 with exceptionally low COX-1 signals in FaDu and HT-29 cells. To differentiate between the specific contribution of COX-1 and COX-2 the overall tracer uptake and intracellular association tracer uptake were determined, unstimulated human monocytes (THP-1) were used as model showing no or very low baseline expression of COX-2.<sup>15,26,27</sup> In contrast, TPA-stimulated THP-1 cells as well as human tumor cell lines FaDu, HT-29, and A2058 served as models for upregulated COX-2 expression (Fig. 2).<sup>28,29</sup>

In the literature, the human malignant melanoma cell line A375 also has been described as COX-2 overexpressing cell line.<sup>29</sup> In contrast, the present investigation showed no or only very low COX-2



**Scheme 4.** Flow diagram of automated radiosynthesis of [ $^{18}\text{F}$ ]-**3** via McMurry cyclization.

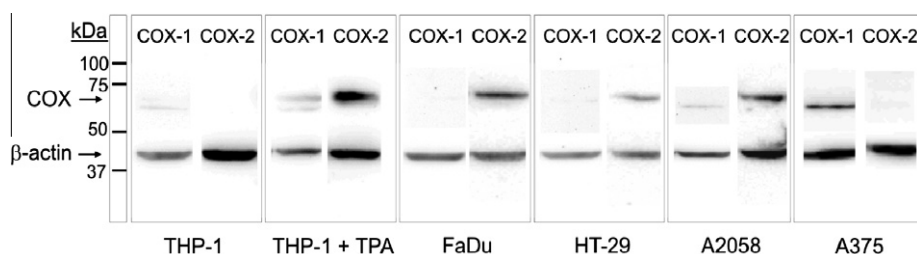


**Figure 2.** Cellular expression of COX proteins in THP-1 and different tumor cell lines detected after SDS-PAGE by Western blotting.

protein expression in A375 cells, but an abundant synthesis of a glycosylated or splice variant of COX-1 (Fig. 2). However, the radiotracer [ $^{18}\text{F}$ ]-**3** uptake data obtained from all cell models used were consistent to the published COX-1/COX-2 selectivity of 3-(4-fluorophenyl)-2-(4-methylsulfonylphenyl)-1*H*-indole **3** (see Fig. 1) and the observed protein expression of COXs.

The *in vitro* cellular uptake and intracellular association of [ $^{18}\text{F}$ ]-**3** in human THP-1 monocytes and differentiated THP-1

macrophages, human tumor cells FaDu, A2058 and A375 and human tumor cell HT-29 monolayers, small- and large-sized spheroids is shown in Figure 3.

Unstimulated THP-1 cells comparatively showed a low uptake, also did A375 cells. Interestingly, radiotracer uptake in A375 cells was substantially higher than in unstimulated THP-1 monocytes although COX protein expression was on a similar level. Of note, in these cells radiotracer uptake was not or only weakly influenced

by preincubation with the nonradioactive reference compound **3**. A possible contribution of the COX-1 variant to overall tracer uptake in A375 cells cannot be excluded. However, COX-2 overexpressing cells showed a drastically increased uptake of [ $^{18}\text{F}$ ]-**3** when compared to cells showing no or only very low COX-2 synthesis. In order to study a regulatory situation with hypoxia-modulated COX-2 expression, uptake of compound [ $^{18}\text{F}$ ]-**3** was studied in multicellular HT-29 spheroids with or without intrinsic hypoxia as model system.<sup>2,30,31</sup> In this model, [ $^{18}\text{F}$ ]FMISO was used to confirm development of intrinsic hypoxia in large-sized spheroids compared to

small-sized spheroids and monolayers, respectively.<sup>32</sup> The [ $^{18}\text{F}$ ]FMISO uptake experiments in HT-29 monolayers ( $1.03 \pm 0.34\% \text{ID}/\text{mg}$  protein) as well as individual HT-29 spheroids with a diameter of both  $300 \pm 10 \mu\text{m}$  ( $1.17 \pm 0.29\% \text{ID}/\text{mg}$  protein) and  $600 \pm 10 \mu\text{m}$  ( $9.86 \pm 3.4\% \text{ID}/\text{mg}$  protein) clearly confirmed development of an intrinsic hypoxia in large-sized spheroids that is high enough to trap [ $^{18}\text{F}$ ]FMISO ( $p\text{O}_2 < 10 \text{ mm Hg}$ ). In consequence of hypoxia-induced stimulation of COX-2 expression in HT-29 spheroids, large-sized spheroids also showed a substantially higher uptake [ $^{18}\text{F}$ ]-**3** when compared to small-sized spheroids and monolayers, respectively. The specificity of the radiotracer uptake was further tested by performing blocking experiments with all cells after preincubation with a  $100 \mu\text{mol/L}$  solution of the corresponding nonradioactive reference compound **3** for 30 min (Fig. 3). Moreover, the possible interaction with the P-glycoprotein (P-gp) efflux pump was examined in the presence of P-gp inhibitor cyclosporine A and the calcium blocker verapamil, respectively.<sup>14,33,34</sup> Therefore, cells were incubated with cyclosporine A and verapamil for 60 min before [ $^{18}\text{F}$ ]-**3** was added to the loading buffer. Accordingly, a decrease in [ $^{18}\text{F}$ ]-**3** cellular uptake or efflux may be an outcome of P-gp interaction. However, both cyclosporine A and verapamil, compared with the control, did not induce any significant effect on [ $^{18}\text{F}$ ]-**3** overall uptake in either cell line and time group (data not shown).

Treatment of HT-29, FaDu and A375 cells with the corresponding nonradioactive reference compound **3** at pharmacological

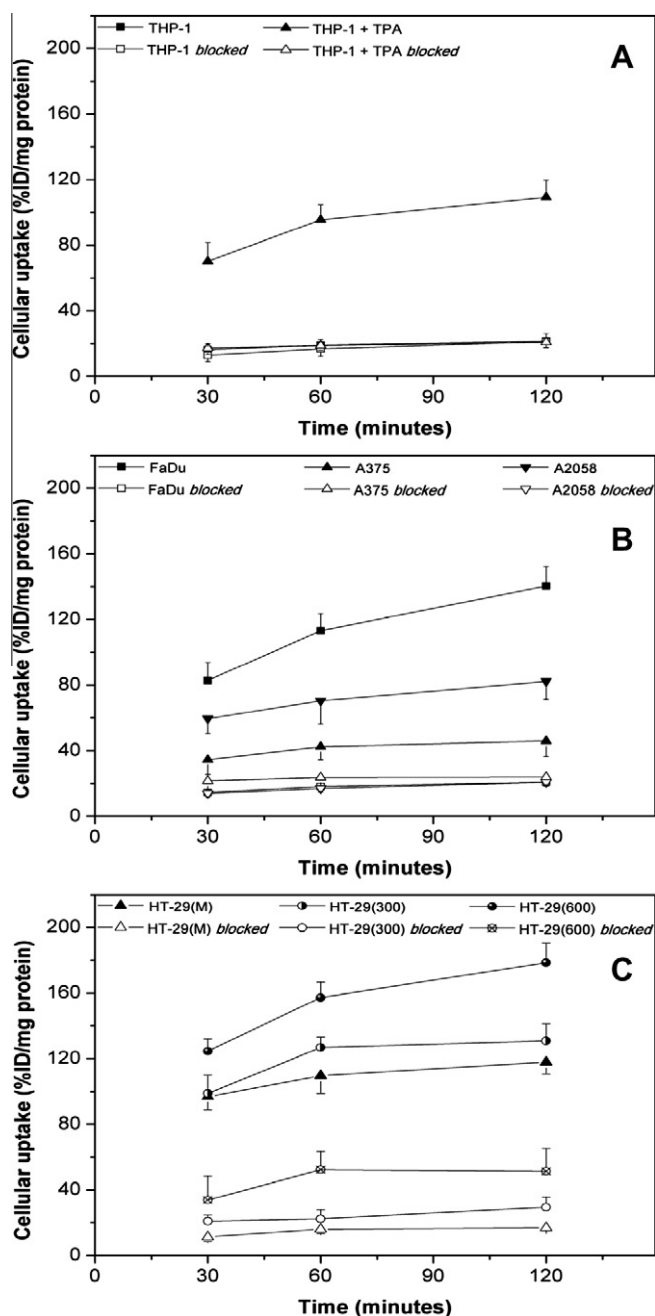


**Figure 3.** In vitro study on overall cellular uptake and intracellular association of [ $^{18}\text{F}$ ]-**3** in human THP-1 monocytes and differentiated THP-1 macrophages (A), human tumor cells FaDu, A2058 and A375 (B), and human tumor cell HT-29 monolayers, small- and large-sized spheroids (C). Results are given as mean  $\pm$  SD ( $n = 6$ ). TPA, stimulation by  $64 \text{ nM}$  phorbol myristate acetate (TPA) for 72 h; blocked, preincubation (for 30 min) with a  $100 \mu\text{mol/L}$  solution of the corresponding nonradioactive reference compound **3**; (M), monolayer; (300), spheroid diameter of  $300 \pm 10 \mu\text{m}$ ; (600), spheroid diameter of  $600 \pm 10 \mu\text{m}$ .

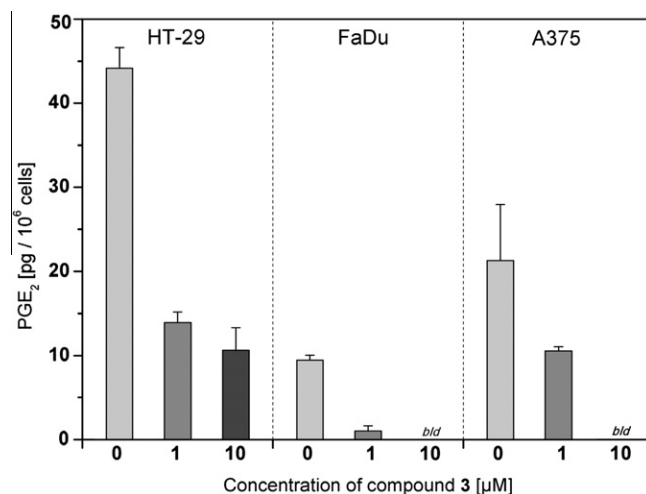


**Figure 4.** LC-MS/MS analysis of PGE<sub>2</sub> in cell culture supernatants of three tumor cell lines incubated with or without compound **3** for 25 h. Concentrations of compound **3** were  $1 \mu\text{M}$  or  $10 \mu\text{M}$ . Data are expressed as  $\text{pg}/10^6$  cells (means  $\pm$  standard deviation),  $n = 6$  from two independent experiments. bld, below limit of detection. The limit of detection was ascertained at  $15 \text{ pM}$ .

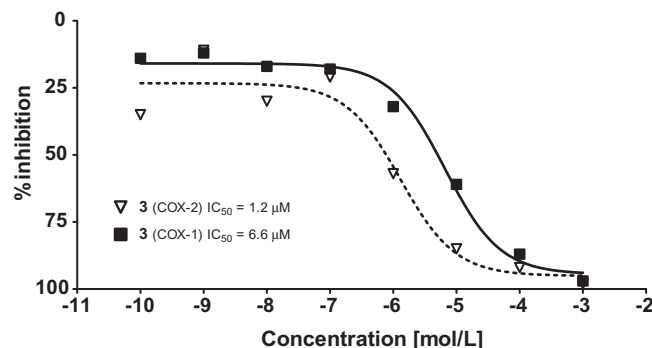


**Figure 5.** Curve of inhibition of **3** for COX-1 and COX-2.

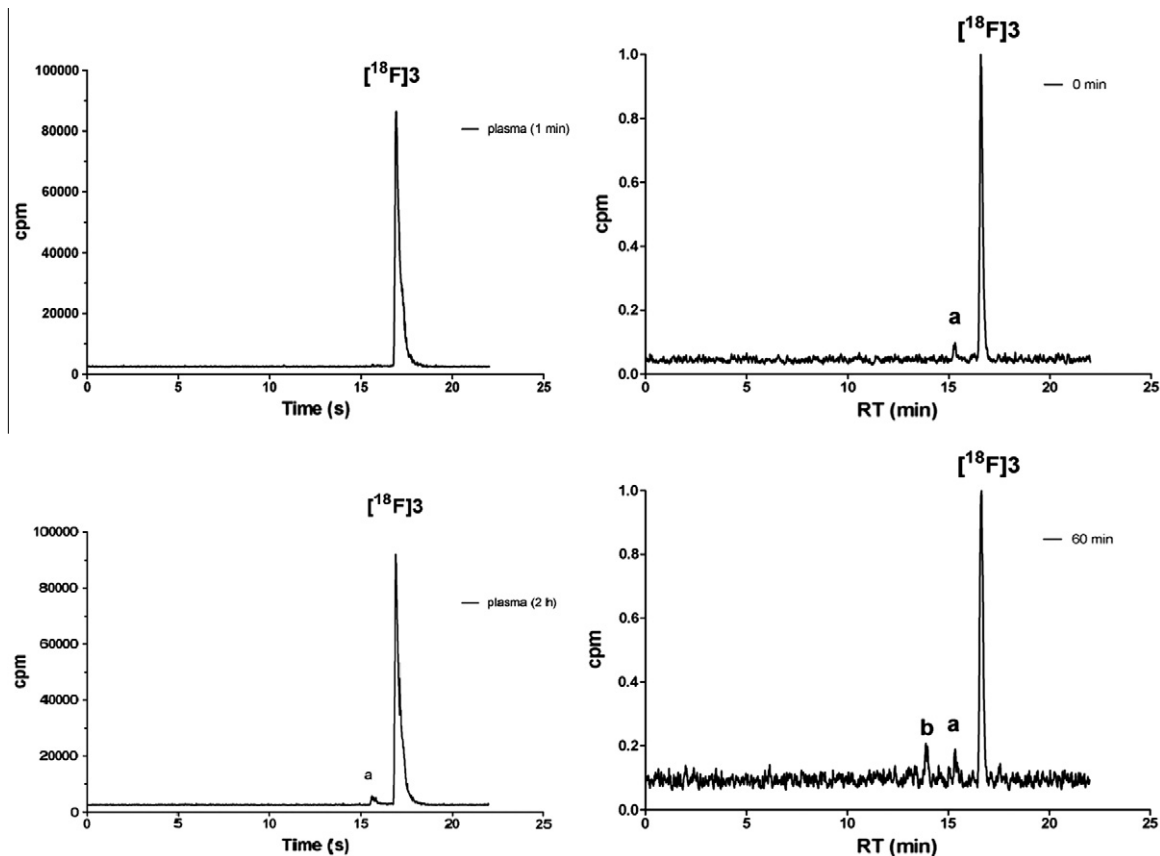


**Figure 6.** Radio-HPLC chromatogram of [ $^{18}\text{F}$ ]-**3** in rat blood plasma after 1 min and 2 h in vitro incubation at 37 °C (left) and of rat arterial plasma samples immediately after intravenous injection and 60 min p.i. (right), metabolites are marked as a and b.

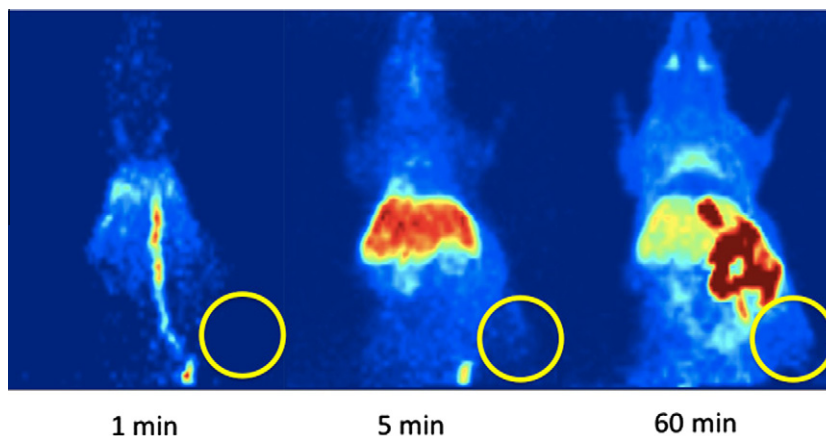


**Figure 7.** Representative small animal PET images of a HT-29 tumor bearing mouse (maximum intensity projections) at 1, 5, and 60 min after single intravenous injection of [ $^{18}\text{F}$ ]-**3**; (circle—position of the subcutaneously xenotransplanted tumor).

concentrations resulted in substantial inhibition of  $\text{PGE}_2$  synthesis in all cell lines (by 52–89% at 1  $\mu\text{M}$ ; by 79–100% at 10  $\mu\text{M}$ ; 100% inhibition equals to *below limit of determination (bld)*) independent on their individual COX expression levels (Fig. 4).

$\text{PGE}_2$  is one of the major metabolites of arachidonic acid synthesized by both cyclooxygenase isoforms. The determination of  $\text{PGE}_2$  level in cell culture supernatants is therefore a direct measure of the COX activity. The cellular inhibition assay results demonstrated the compound **3** to be a potent cyclooxygenase inhibitor, however, also point to an only low COX-1/COX-2 selectivity of compound **3**. In order to further evaluate the actual selectivity of **3**, the

compound was applied to an enzymatic competitive inhibition assay with celecoxib as reference compound. By using this assay in our laboratories the inhibitory potency for **3** ( $\text{IC}_{50}$ ) was determined to be 6.6  $\mu\text{M}$  for COX-1 and 1.2  $\mu\text{M}$  for COX-2 (Fig. 5) while for celecoxib  $\text{IC}_{50}$  values of 115  $\mu\text{M}$  (COX-1) and 0.06  $\mu\text{M}$  (COX-2) were found. Of note, the data measured for compound **3** result in a low COX-1/COX-2 selectivity ratio of 5.5 and are in a strong contradiction to the primary presumed selectivity ratio of 500 for compound **3** that has been published in the literature.<sup>13</sup> Nevertheless, the overall results demonstrated that [ $^{18}\text{F}$ ]-**3** is a suitable indicator of increased COX-2 expression in conditions associated with

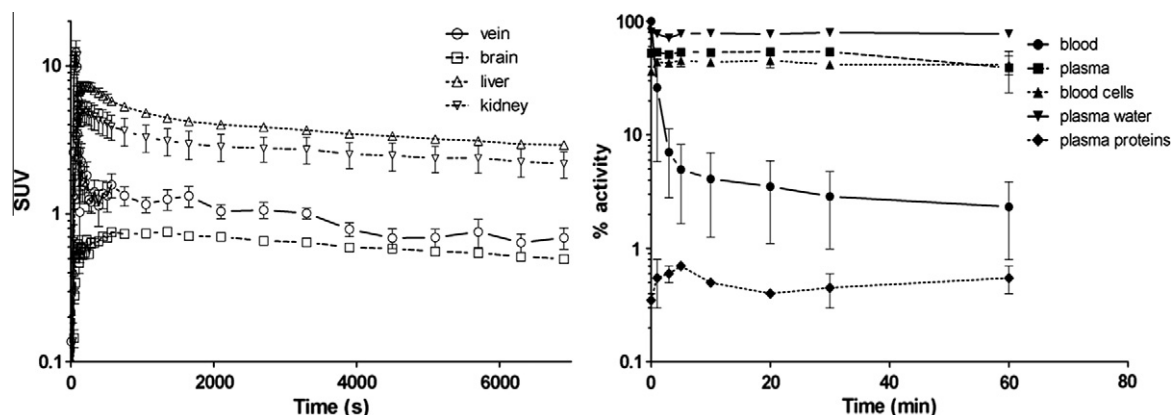


**Figure 8.** Time activity curves. Left:  $^{18}\text{F}$ -activity in the blood (vein, ROI over the abdominal vena cava and aorta), brain, liver and kidney measured with PET. Data are means  $\pm$  SEM of 9 mice. Right: external measured arterial blood  $^{18}\text{F}$ -activity (% of maximum activity) and the relative (% of activity) distribution of the  $^{18}\text{F}$ -activity between the blood components (blood cells, plasma proteins, plasma water). Data are means  $\pm$  SEM of blood samples of two rats.

inflammatory, tumorigenic or hypoxia-related stimuli *in vitro*. Thus, the results showed promise for evaluating [ $^{18}\text{F}$ ]-**3** as a positron-emitting probe for imaging of distribution or functional expression of COX-2 by PET in HT-29 tumor xenotransplanted mice.

### 3.5. Stability studies *in vitro* and *in vivo*

The *in vitro* stability of [ $^{18}\text{F}$ ]-**3** was determined by incubation in rat whole blood and plasma for 1 min and 2 h at 37 °C, respectively. In all analyses only one more polar metabolite (**a**) in very small amounts (lower 5% of activity) was observed after 2 h (Fig. 6).

A similar metabolic behavior was observed *in vivo*. Metabolite analysis of arterial blood samples with radio-HPLC after intravenous injection of the radiotracer into rats indicated that a minor part of [ $^{18}\text{F}$ ]-**3** was rapidly converted immediately after application into the more polar metabolite (**a**), amounting to about 5% of the applied activity at 5 min after injection. After 60 min a second more hydrophilic radioactive metabolite (**b**) could be detected and the original compound [ $^{18}\text{F}$ ]-**3** in rat plasma still amounted to 75% with the two metabolites **a** (12.3%) and **b** (13.7%) comprising 25% of the applied (decay corrected) activity (Fig. 6).

### 3.6. Small animal PET studies

To further assess the feasibility of compound [ $^{18}\text{F}$ ]-**3** as PET radiotracer for imaging COX-2, particularly, COX-2 overexpressing tumors, small animal PET imaging was performed in HT-29 tumor-bearing mice. In the small animal PET experiments, 20 MBq of [ $^{18}\text{F}$ ]-**3** was administered intravenously into the tail vein (corresponding to 0.1  $\mu\text{g}$  (0.28 nM) of **3**). In contrast to the *in vitro* experiments, the small animal PET studies showed no substantial accumulation of [ $^{18}\text{F}$ ]-**3** in human colorectal adenocarcinoma (HT-29) xenotransplanted in nude mice. Dynamic PET studies revealed that the main activity was fast accumulated in the liver and was eliminated by the hepatobiliary route into the intestine (Fig. 7). A substantial amount of activity was accumulated in the Harderian glands and the brown adipose tissue. The kidneys showed a temporary accumulation of minor part of the activity. A very low amount of activity temporarily could be detected in the brain.

The clearance of the activity in mice from the blood (ROI over the abdominal part of the *vena cava* and *aorta*), liver, kidneys and brain were similar (Fig. 8). The main activity was eliminated into the intestine. For comparison, in rats the arterial blood clearance was externally measured as shown in Figure 6. The half-life of

the elimination phase was, similar to the situation in mice, very short with 8.2 min calculated using a two-phase elimination model. These data indicate that [ $^{18}\text{F}$ ]-**3** is not suitable for functional imaging of COX-2 in rodent models *in vivo*.

The reasons for that behavior are manifold; mainly the affinity of **3** for COX-2 is with 1.2  $\mu\text{M}$  not specific enough to address the target enzyme, for that purpose an affinity in the nanomolar range is required. On the other hand, the low COX-1/COX-2 selectivity ratio may result in a substantial binding of the radiotracer in the multitude of cells constitutively expressing COX-1, this also could contribute to the observed lower overall availability of [ $^{18}\text{F}$ ]-**3** in the HT-29 tumor. Furthermore, it can be hypothesized that the perfusion of the tumors in the model used was too low for significant intracellular tracer accumulation and that the lipophilic profile of [ $^{18}\text{F}$ ]-**3** is not optimal for crossing the cell membrane and is responsible for high unspecific binding in nontargeted tissues such as the gastrointestinal tract, liver, and kidneys. On the other hand, an important criterion for a 'successful' radiotracer is a high specific radioactivity. The specific radioactivity should be as high as possible to minimize a binding competition between radiolabeled and non-labeled inhibitor. In case of [ $^{18}\text{F}$ ]-**3** a specific radioactivity ranging from 74 to 91 GBq/ $\mu\text{mol}$  at the end of synthesis was achieved. This results in an administered dose of **3** of 0.1  $\mu\text{g}$  (0.28 nM) that should be adequate low not to compete with the radiotracer.

## 4. Summary and concluding remarks

The aim of the present work was to develop an  $^{18}\text{F}$ -radiolabeled cyclooxygenase inhibitor with the scaffold of a diarylsubstituted indole exhibiting high affinity and selectivity towards COX-2. Because a direct nucleophilic substitution with  $^{18}\text{F}$ -fluoride on the lead structure was not very promising, we used a specially designed benzophenone **9** with a trimethylammonium leaving group as precursor molecule for introduction of the radiolabel. The radiotracer [ $^{18}\text{F}$ ]-**3** was synthesized by cyclization of the intermediate [ $^{18}\text{F}$ ]-**4** with low valent titanium and zinc by application of the McMurry protocol from organic synthesis onto radiochemistry. In this manner [ $^{18}\text{F}$ ]-**3** was synthesized via a two-step procedure in a remote controlled synthesizer unit covering purification, solid phase extraction and formulation for radio pharmacological investigation in 10% total decay corrected yield with high radiochemical purity and a specific activity of 74–91 GBq/ $\mu\text{mol}$  at EOB. Consideration of *in vitro* properties, including affinity and distribution between the blood cells, plasma proteins and water, showed promise for *in vivo* imaging application of the radiotracer [ $^{18}\text{F}$ ]-**3**.

However, although showing micromolar affinity for COX-2 and acceptable high metabolic blood stability in vivo, [ $^{18}\text{F}$ ]-**3** turned out to be not suitable for in vivo imaging of COX-2 in mice with xenotransplanted HT-29 tumors. It should be pointed out that the high specificity and selectivity data of **3** published in the literature<sup>13</sup> prompted us in the development of the radiotracer [ $^{18}\text{F}$ ]-**3** as a lead compound. However in the present study two independent COX-2 activity assays demonstrated only a low selectivity of **3** for COX-2 at pharmacological concentrations.

Nevertheless, from a radiochemical point of view it should be underlined that the utilization of McMurry cyclization gives access to  $^{18}\text{F}$ -labeled diarylsubstituted indoles, a class of compounds that is by conservative labeling techniques not straightforward available so far. In our ongoing work a sequence of further 2,3-diaryl-substituted indoles and similar five and six-membered nitrogen containing heterocycles is under preparation and will be evaluated as new inhibitors of COX-2. The compounds showing the best affinity, selectivity, and most promising bioavailability will be subjected  $^{18}\text{F}$ -radiolabeling to further in vivo functional characterization of cyclooxygenases.

### Acknowledgements

The authors wish to thank S. Preusche for radioisotope production and M. Barth, C. Heinig, R. Herrlich, S. Lehnert, A. Suhr and P. Wecke for expert technical assistance in the chemical and radiopharmacological investigations.

### References and notes

- Blombaum, A. L.; Marnett, L. J. *J. Med. Chem.* **2007**, *50*, 1425.
- Greenhough, A.; Smartt, H. J.; Moore, A. E.; Roberts, H. R.; Williams, A. C.; Paraskeva, C.; Kaidi, A. *Carcinogenesis* **2009**, *30*, 377.
- Wang, D.; BuBois, R. N. *Nat. Rev. Cancer* **2010**, *10*, 181.
- Rizzo, M. T. *Clin. Chim. Acta* **2011**, *412*, 671.
- Chakraborti, A. K.; Garg, S. K.; Kumar, R.; Motiwala, H. F.; Jadhavar, P. S. *Curr. Med. Chem.* **2010**, *17*, 1563.
- Kao, J.; Genden, E. M.; Chen, C. T.; Rivera, M.; Tong, C. C.; Misiukiewicz, K.; Gupta, V.; Gurudutt, V.; Teng, M.; Packer, S. H. *Cancer* **2011**, *117*, 3173.
- De Vries, E. F. *Curr. Pharm. Des.* **2006**, *12*, 3847.
- Prabhakaran, J.; Underwood, M. D.; Parsey, R. V.; Arango, V.; Majo, V. J.; Simpson, N. R.; van Heertum, R.; Mann, J. J.; Kumar, J. S. D. *Bioorg. Med. Chem.* **1802**, *2007*, 15.
- De Vries, E. F.; Doorduyn, J.; Dierckx, R. A.; van Waarde, A. *Nucl. Med. Biol.* **2008**, *35*, 35.
- Uddin, J.; Crews, B. C.; Ghebreselaise, K.; Huda, I.; Kingskey, P. J.; Sib Ansan, M.; Tantawy, M. N.; Reese, J.; Marnett, L. J. *Cancer Prev. Res.* **2011**, *4*, 1536.
- Wuest, F. R.; Hoehne, A.; Metz, P. *Org. Biomol. Chem.* **2005**, *3*, 503.
- Wuest, F.; Kniess, T.; Bergmann, R.; Pietzsch, J. *Bioorg. Med. Chem.* **2008**, *16*, 7662.
- Hu, W.; Guo, Z.; Chu, F.; Bai, A.; Yi, X.; Cheng, G.; Li, J. *Bioorg. Med. Chem.* **2003**, *11*, 1153.
- Tanaka, M.; Fujisaki, Y.; Kawamura, K.; Ishiwata, K.; Qinggeletu; Yamamoto, F.; Mukai, T.; Maeda, M. *Biol. Pharm. Bull.* **2006**, *29*, 2087.
- Buu-Hoi, L. *Bull. Soc. Chim. Fr.* **1946**, 139.
- Coombs, R. V.; Danna, R. P.; Denzer, M.; Hardtmann, G. E.; Huegi, B.; Koletar, G.; Koletar, J.; Ott, H.; Jukniewicz, E. *J. Med. Chem.* **1973**, *16*, 1237.
- Tang, G.; Wang, M.; Tang, X.; Gan, L.; Luo, L. *Nucl. Med. Biol.* **2005**, *32*, 553.
- Cao, H.; Xiao, L.; Park, G.; Wang, X.; Azim, A. C.; Christman, J. W.; van Breemen, R. B. *Anal. Biochem.* **2008**, *372*, 41.
- Schütze, C.; Bergmann, R.; Yaromina, A.; Hessel, F.; Kotzerke, J.; Steinbach, J.; Baumann, M.; Beuthien-Baumann, B. *Radiother. Oncol.* **2007**, *83*, 311.
- McMurry, J. E. *Chem. Rev.* **1989**, *89*, 1513.
- Lee, B. C.; Lee, K. C.; Lee, H.; Mach, R. H.; Katzenellenbogen, J. A. *Bioconjugate Chem.* **2007**, *18*, 507.
- Kudav, D. P.; Samant, S. P.; Hosangadi, B. D. *Synth. Commun.* **1987**, *17*, 1185.
- Hamacher, K.; Hamkens, W. *Appl. Radiat. Isot.* **1995**, *46*, 911.
- Chandrasekharan, N. V.; Dai, H.; Roos, K. L.; Evanson, N. K.; Tomsik, J.; Elton, T. S.; Simmons, D. L. *Proc. Natl. Acad. Sci. U.S.A.* **2002**, *99*, 13926.
- Schumacher, K.; Castrop, H.; Strehl, R.; de Vries, U.; Minuth, W. W. *Cell. Physiol. Biochem.* **2002**, *12*, 63.
- Bagga, D. W.; Wang, L.; Farias-Eisner, R.; Glaspy, J. A.; Reddy, S. T. *Proc. Natl. Acad. Sci. U.S.A.* **2003**, *100*, 1751.
- Goppelt-Strube, M.; Schaefer, D.; Habenicht, A. J. *Br. J. Pharmacol.* **1997**, *122*, 619.
- Lev-Ari, S.; Strier, L.; Kazanov, D.; Madar-Shapiro, L.; Dvory-Sobol, H.; Pinchuk, I.; Marian, B.; Lichtenberg, D.; Arber, N. *Clin. Cancer Res.* **2005**, *11*, 6738.
- Denkert, C.; Köbel, M.; Berger, S.; Siegert, A.; Leclere, A.; Trefzer, U.; Hauptmann, S. *Cancer Res.* **2001**, *61*, 303.
- Lee, J. J.; Natsuizaka, M.; Ohashi, S.; Wong, G. S.; Takaoka, M.; Michaylira, C. Z.; Budo, D.; Tobias, J. W.; Kanai, M.; Shirakawa, Y.; Naomoto, Y.; Klein-Szanto, A. J.; Haase, V. H.; Nakagawa, H. *Carcinogenesis* **2010**, *31*, 427.
- Kaidi, A.; Qualtrough, D.; Williams, A. C.; Paraskeva, C. *Cancer Res.* **2006**, *66*, 6683.
- Rasey, J. S.; Nelson, N. L.; Chin, L.; Evans, M. L.; Grunbaum, Z. *Radiat. Res.* **1990**, *122*, 301.
- Herzog, C. E.; Trepel, J. B.; Mickley, L. A.; Bates, S. E.; Fojo, A. T. *J. Natl. Cancer Inst.* **1992**, *84*, 711.
- Beck, W. T.; Qian, X. D. *Biochem. Pharmacol.* **1992**, *43*, 89.